Development/Plasticity/Repair

Mechanisms of Dendritic Elaboration of Sensory Neurons in *Drosophila*: Insights from *In Vivo* Time Lapse

Darren W. Williams and James W. Truman
Department of Biology, University of Washington, Seattle, Washington 98195

In vivo **time-lapse multiphoton microscopy was used to analyze the remodeling of the dendritic arborizing (da) sensory neuron known as dorsal dendritic arborizing neuron E (ddaE) during metamorphosis. After its larval processes have been removed, the cell body of ddaE repositions itself on the body wall between 25 and 40 hr after puparium formation (APF) and begins its adult outgrowth at 40 hr APF. The scaffold of the arbor is laid down between 40 and 54 hr APF, when growth is characterized by high filopodial activity at both terminal and interstitial positions and by branch retraction along with branch establishment. Later in development, filopodial activity remains high but is confined to terminal branches, and branch retraction is no longer seen. Treatment with the insect hormone juvenile hormone (JH), a key regulator of metamorphosis, alters the shape and complexity of the adult dendritic tree in a time-dependent manner. Early treatments with juvenile hormone mimic (JHm) appear to repress extension programs and maintain retraction programs. With later JHm treatments, extension programs appear normal, but retraction programs are maintained beyond their normal time. The JH treatments show the importance of retraction programs in establishing the overall arbor shape.**

Key words: Drosophila; **metamorphosis; multiphoton microscopy; dendrites; juvenile hormone (JH); sensory neuron**

Introduction

Dendrites are the major sites of input into neural networks, first receiving and then integrating information. The mature forms of dendritic arbors have been described in great detail since the time of Santiago Ramon y Cajal, and yet we still know little about the underlying developmental mechanisms that generate these complex structures (for review, see Jan and Jan, 2001; Scott and Luo, 2001; Miller and Kaplan, 2003).

The two key characters that vary consistently among the dendrites of all taxa are arbor complexity (i.e., the degree of branching) and the territory occupied within the neuropil or sensory field. Both characters are critically important in dictating the role a cell will play within a network. Dendrites can be refined by experience and learning throughout the life of the organism (Trachtenberg et al., 2002; Leuner et al., 2003), but the fundamental shape is established during a discrete developmental period through the execution of cell-intrinsic programs (Grueber et al., 2003a; Komiyama et al., 2003) and extrinsic interactions with other cells in their immediate environment (Rakic and Sidman, 1973; Grueber et al., 2003b).

From a number of studies, it is clear that the growth of a dendritic arbor can be broken down into a series of steps. These begin with the directed growth of the primary dendrite to the target field followed by branching of the growth cone to generate a basic scaffold within that field. The scaffold is then elaborated on with the growth of higher-order branches. Outgrowth eventually slows, the major branches become stable, and the arbor is refined (Shepherd and Laurent, 1992; Wu et al., 1999).

Here, we describe the dynamic structural changes underlying the metamorphic reorganization of abdominal sensory neurons in live intact *Drosophila* using *in vivo* time-lapse multiphoton microscopy. We observed the migration and outgrowth of the adult arbor of persistent larval dendritic arborizing (da) sensory neurons.

The developmental hormones that orchestrate metamorphosis are 20-hydroxyecdysone (20E) and juvenile hormone (JH) (Riddiford, 1993). JH micromanages the response of a cell to 20E (Riddiford, 1976; Zhou et al., 1998). We use juvenile hormone as a tool to define two phases of dendritic outgrowth. These data suggest that the type of growth associated with the early phase may be important for generating the scaffold, and that exiting this mode is essential for generating an arbor of appropriate complexity.

Materials and Methods

Fly stocks. For all live imaging experiments, we used a stable line containing the *C161-GAL4* driver (Shepherd and Smith, 1996) with two copies of the *UAS-mCD8::GFP* reporter (Lee and Luo, 1999). For mosaic analysis with a repressible cell marker (MARCM) (Lee and Luo, 1999) of da sensory neurons, the following genotype was generated: *19A FRT/hsFLP, tub-GAL80, 19A FRT*; *UAS-mCD8::GFP/+*; *C161-GAL4, UAS-mCD8::GFP/+*.

Lineage analysis. MARCM clones were induced in the embryo by a double heatshock method (Grueber et al., 2002). Flies were allowed to lay eggs on yeasted grape juice plates at 25°C for 2 hr. The embryos were then allowed to develop for 4 hr at 25°C. Embryos were then given a 30 min heatshock at 37°C, a 30 min recovery period at 25°C, and then another 45 min heatshock at 37°C. These animals were grown to the third instar and

Received Oct. 4, 2003; revised Nov. 21, 2003; accepted Nov. 29, 2003.

Research was funded by National Institutes of Health Grant RO1 NS13979. We thank Todd Clason for technical support, Lynn Riddiford for reagents and advice on JH applications, and Margrit Schubiger for critical reading of this manuscript.

Correspondence should be addressed to Darren W. Williams, Department of Biology, University of Washington, Kincaid Hall Box 351800, Seattle, WA 98185-1800. E-mail: dww@u.washington.edu.

DOI:10.1523/JNEUROSCI.4521-03.2004

 0270-6474/04/241541-10$15.00/0

screened for single-neuron clones in the periphery under epifluorescence. Larvae with clones were anesthetized with ether, and the neuron was imaged through the body wall using confocal microscopy. The larva was subsequently allowed to pupariate. Later, the pupa was removed from its puparial case, and the same neuron was imaged again at ~72 hr after puparium formation (APF) with confocal microscopy.

Staging of animals. Individual animals were collected at pupariation and maintained at 25°C in a Petri dish with moist filter paper. Staging was denoted as hours after puparium formation.

Hormone application. The juvenile hormone mimic (JHm) pyriproxifen (Sumitomo Chemical, Osaka, Japan) was dissolved in acetone and applied using a 10 μl Hamilton syringe to whole prepupae or to pupae after the operculum of the puparial case had been removed. Each animal received a dose of 100 ng in 0.2 μl of acetone.

Wax containing JHm was made by mixing pyriproxifen in acetone with melted dental wax to a concentration of 0.2 μg/μl. Individual pupae were removed from their puparial case, and a drop of melted wax measuring ~500 μm in diameter was applied onto the pupal cuticle using a bent insect pin. Pupae were maintained at 25°C in a Petri dish with moist filter paper.

Image acquisition. Individual staged animals were dissected out of their puparial cases and placed in an imaging chamber. The imaging chamber (Kiehart et al., 1994) consisted of a slide with a hole over which an oxygen-permeable membrane (standard membrane, model 5793; YSI, Yellow Springs, OH) was held in place with an O ring. A wall of silicon grease was built on the membrane around the pupa, and a coverslip was fixed on top with dental wax to prevent movement in the *z*-axis. Pupae could be imaged from 14 hr APF to the pharate adult stage. Complete adult development takes place within the chamber, and the control adults can eclose from their pupal cuticle.

Single images of green fluorescent protein (GFP)-expressing da neurons were taken by confocal microscopy using a Bio-Rad (Hercules, CA) Radiance 2000 System equipped with a krypton–argon laser set at 488 nm, with a Nikon (Tokyo, Japan) Eclipse E600FN microscope with a 40×/1.3 Nikon Plan Apo oil objective. Individual pupa were kept in saline under a coverslip held in place using dental wax.

Time-lapse images were acquired using the same Bio-Rad Radiance 2000 System equipped with a Mai Tai laser (Spectra-Physics, Fremont, CA) set at 905 nm and a Nikon Eclipse E600FN microscope with a 40×/1.3 Nikon Plan Apo oil objective. Data were collected using the Direct Detection System and LaserSharp software (Bio-Rad). During time-lapse recordings, each time point consisted of a z-stack of ~22 sections at 1.5 μm intervals.

Image analysis. Stacks and movies (available at www.jneurosci.org) were assembled in NIH Image J (http://rsb.info.nih.gov/ij/). Images were adjusted only for brightness and contrast using Adobe Photoshop (Adobe Systems, San Jose, CA).

A quantitative measure of complexity was obtained using Sholl analysis (Sholl, 1953). The number of intersections between dendritic processes and sequential Sholl rings was counted and displayed using a spectral color code. Intersections were determined in Photoshop using a template of 12 concentric red circles with diameters increasing in increments of 12 μm laid over a single projected z-stack of an individual arbor. The exclusion function in the layers menu was used to show intersections in turquoise.

Branch analysis was performed on timeline data sets that had been printed onto letter-sized paper. Individual acetate sheets were placed onto these images, and colored pens were used to denote branch birth. After the analysis, the branches were drawn onto the original projected z-stack using Canvas (version 5.0; ACD Systems, British Columbia, Canada).

Results

Metamorphic reorganization of da sensory neurons

da sensory neurons have complex peripheral arbors that cover the body wall of *Drosophila* larvae to generate nonredundant overlapping sensory systems (Grueber et al., 2002). During metamorphosis, the majority of larval sensory neurons die, except for a small number that persist to become functional adult neurons (Williams and Shepherd, 1999). Some da neurons are among those that persist through metamorphosis, and their axons serve as guides for the ingrowth of adult sensory neurons (Usui-Ishihara et al., 2000; Williams and Shepherd, 2002). In their adult form, they establish elaborate dendritic arbors that spread over the epidermis (Smith and Shepherd, 1996). One especially prominent da neuron is located under the lateral tergite of abdominal segments 2–5 and has a large radial arbor (Fig. 1*A*,*B*). Data from four different GAL4 drivers, including da driver *109(2)80*, which expresses in all dendritic arborizing neurons (Gao et al., 1999), show that its arbor does not overlap that of any other da neuron (data not shown).

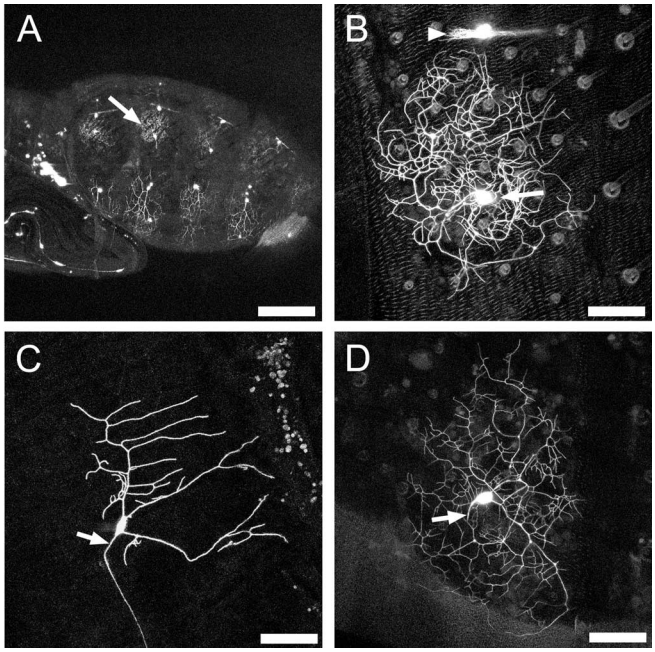

Figure 1. Morphology of the dendritic arborizing neuron ddaE. *A*, Lateral view of the abdomen of a pharate adult. The projected confocal z-stack of *C161-GAL4* driving *UAS-CD8::GFP* shows internal sensory neurons in the periphery of the pharate adult abdomen. ddaE (arrow) is located under the lateral region of the tergite. Scale bar, 220 μm. Anterior is to the left, and dorsal is up. *B*, Detail of *C161-GAL4* driving *UAS-CD8::GFP*. A projected confocal z-stack shows the detail of dbd (arrowhead) and ddaE (arrow). Dorsal is up, and anterior is to the left. The bristles and trichomes on the overlying tergite are visible. Scale bar, 40 μm. *C*, Projected confocal z-stack of a single-neuron MARCM clone of ddaE imaged live in third instar larva. The axon is labeled with an arrow. Scale bar, 85 μm. *D*, Projected confocal z-stack of the same neuron as in *C* imaged live at ~72 hr APF. The axon is labeled with an arrow. Scale bar, 45 μm.

To establish that this dorsolateral da neuron was indeed a remodeled larval sensory neuron, we generated MARCM clones with the GAL4 enhancer trap line *C161*. This line expresses in a subset of the da neurons in both larvae and adults (Shepherd and Smith, 1996; Smith and Shepherd, 1996). GFP-labeled MARCM clones were induced by heatshock of early embryos, and we then screened third instar larvae for individuals that had single da neurons expressing GFP. These larvae were lightly anesthetized, the neuron was imaged, and the larva was then allowed to pupariate. The same neuron was then imaged ~72 hr after pupariation. Figure 1, *C* and *D*, shows the same neuron from the same individual in its larval and adult form. On the basis of its larval form, this cell can be identified as dorsal dendritic arborizing neuron E (ddaE) (Grueber et al., 2002), and we also used that name for the adult form of the cell. In the larva, ddaE is assigned a type I classification (Grueber et al., 2002). This class of da neuron has

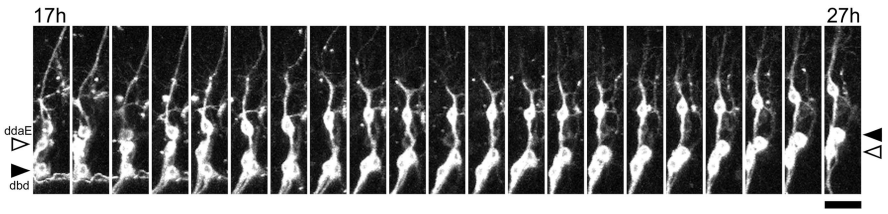

Figure 2. Change in position of sensory neurons on the abdominal peripheral nerve. Single frames from a time-lapse movie show changes in the relative position of ddaE and dbd between 17 and 27 hr APF. Frames are at 30 min intervals of neurons expressing the *CD8::GFP* reporter. During this time, the cell bodies of ddaE (white arrowhead) and dbd (black arrowhead) change their relative positions on the peripheral nerve before they both migrate dorsally. Scale bar, 50 μm.

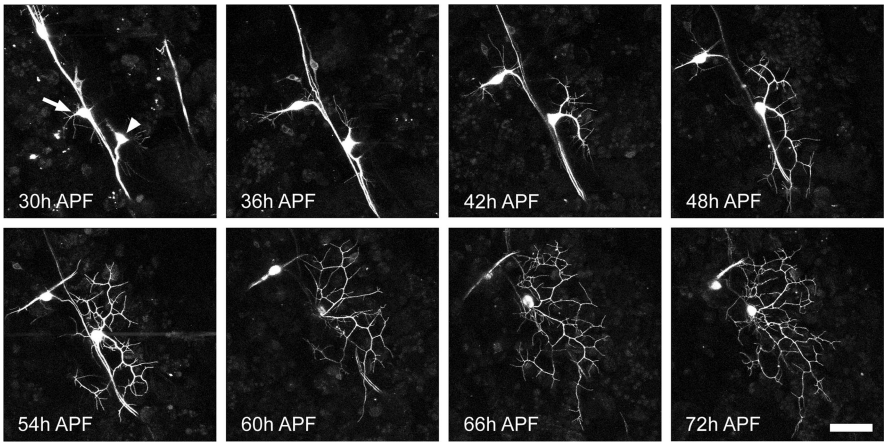

Figure 3. Outgrowth of adult dendritic arbor of ddaE. A projection of multiphoton z-stacks of a neuron expressing the CD8::GFP reporter, from a single pupa, imaged every 6 hr between 30 and 72 hr APF is shown. Acetone was applied at 24 hr APF. At 30 hr APF, the larval dendrites have been completely removed and the cell bodies of ddaE (arrowhead), dbd (arrow), and two other da neurons migrate up the body wall. At 36 hr APF, the growth cones are simple with only a few filopodia extending from short primary dendrites. Between 42 and 48 hr APF, the arbor increases in complexity and size. Between 54 and 72 hr APF, the basic scaffold was elaborated on with higher-order branches. Scale bar, 40 μm.

the simplest arbor of all classes of larval da neurons. As seen in Figure 1*D*, the adult morphology of ddaE is significantly more complex. Single-cell clones of ddaE in two larvae both showed this larval cell transforming into the same adult da neuron.

In assuming its adult form, ddaE appears to change position relative to other persisting sensory neurons, such as the stretch receptor dorsal bipolar dendrite neuron (dbd). In the larva, the cell body of ddaE is located on the nerve root dorsal to dbd, whereas in the adult, it is ventral to this neuron. To confirm that there was indeed a position change of the two cells during metamorphosis, we undertook a time-lapse analysis of cell movement on the peripheral nerve after pupation. As seen in Figure 2, dbd (black arrowhead) and ddaE (white arrowhead) change position relative to one another at ~19 hr APF, which is after the da neurons have pruned back the majority of their larval dendrites and before they grow their adult arbors (see below).

Outgrowth of the adult dendritic arbor

In this paper, we confined our analysis to the outgrowth of ddaE. To establish the major themes in the growth of the adult arbor, we collected z-stacks from the same neuron at 6 hr intervals from 30 to 72 hr APF. At 30 hr APF, the larval dendrites have been completely removed, and the cell body of ddaE has moved close to the peripheral nerve (Fig. 3, 30 hr APF) and migrated dorsally with the stretch receptor dbd and two other da neurons. A small number of filopodia can be seen extending from the cell body. By 36 hr APF, the cell body has nearly reached its final location on the body wall (Fig. 3, 36 hr APF); the growth cones are simple, with only a few filopodia extending from short primary dendrites. Sholl analysis of this and another neuron (Fig. 4*Ai*,*Aii*) shows that at 30 and 36 hr APF, ddaE has its fewest number of processes and covers only a small area of the epidermis. The branch analysis (Fig. 4*B*) also reveals that there is little stability of the processes at this time, with most processes being lost between time points.

Between 42 and 48 hr APF, the arbor undergoes an increase in complexity and size with a rapid expansion over the epidermis (Fig. 3, 42 and 48 hr APF). This change in growth can be clearly seen in the Sholl analysis as both an increase in the overall number of process intersections and an increase in the number of concentric rings that the neuron crosses as it extends over its target field (Fig. 4*Ai*,*Aii*, 42 and 48 hr APF). These time points also represent an important transition in growth, because the branch analysis shows that a number of branches born at this time (i.e., blue and light blue) become stabilized and are still present late in development at 72 hr APF. During this time, the basic scaffold of the arbor is established.

Between 54 and 72 hr APF (Fig. 3, 54–72 hr APF), the scaffold remains stable and is further elaborated on with higher-order branches. As a general trend, the number of intersections of a given ring increases in the Sholl analysis, suggesting that once the scaffold is stabilized, the arbor is then filled in. The changes to individual branches (Figs. 3, 4*B*) show that the growth of higher-order branches is still dynamic with filopodia extending and retracting.

Dynamics of early adult outgrowth

The above analysis shows that ddaE starts to establish its primary adult dendrites between 36 and 40 hr APF. To understand the dynamics of this early dendrite formation, we analyzed multiphoton time-lapse movies taken with sampling intervals of 10 min. Figure 5 starts at 39 hr APF and illustrates the dynamic aspects of growth. The thinnest processes are filipodia that are actin-rich (data not shown). Filopodia are distributed all along the length of the primary dendrite, and the majority of the filopodia turn over between one frame and the next, 10 min later. More frequent sampling (every 2 min) showed that filopodial extension and retraction takes place on a minute time scale (data not shown). Branches appear to be born at interstitial positions where thin processes have remained stable for a number of frames. Between the time points shown in Figure 5, *E* and *F*, a thin process tipped with a growth cone becomes engorged with CD8::GFP. This branch remains until the end of the time-lapse footage and acquires filopodia and higher-order branches. However, some apparently substantial branches are labile at this early stage and may persist for ≥1 hr before they are removed. For example, the left branch in Figure 5*A*, which has ~10 filopodia, is lost within 1 hr. Similarly, the branch labeled with an arrow in Figure 5*G* is lost ~3 hr later. Thus, this early stage of arbor growth is char-

acterized by the production of transient branches as well as active filopodia cycling that are distributed along the entire length of the primary dendrites (also see movie 1, available at www.jneurosci.org).

Dynamics of late growth of the adult arbor

To obtain a better understanding of the late growth of the arbor of ddaE, time-lapse movies were initiated at 48 hr APF, with samples taken every 30 min for a period of 24 hr. Figure 6 shows the details of one of these movies. Filopodia are abundant and can be seen in every frame of this movie (arrowheads). An arrow labels a stable branch in the first frame, which remains intact throughout the entire time-lapse sequence. At 55.5 hr APF, a new branch is initiated at a site where there has been filopodial activity and a growth cone has formed. Once established, this new branch is stabilized, and higher-order branches are generated on it (Fig. 6, arrow, 55.5 hr APF). Through this period, we found no instance of the loss of a substantial branch. Although showing the high filopodial activity seen in the earlier phase of growth, this late phase of growth is characterized by branch stability (movie 2, available at www.jneurosci.org). Also, filopodial cycling appears to be confined to the ends of branches and is absent from interstitial areas (i.e., between branch nodes) of stable lower-order branches. For a second-order branch with five third-order branches on it, see Figure 13*E*. Between 58 and 72 hr APF, only a single filopodium was observed, extending from the interstitial region on this entire branch (see Fig. 13*D*).

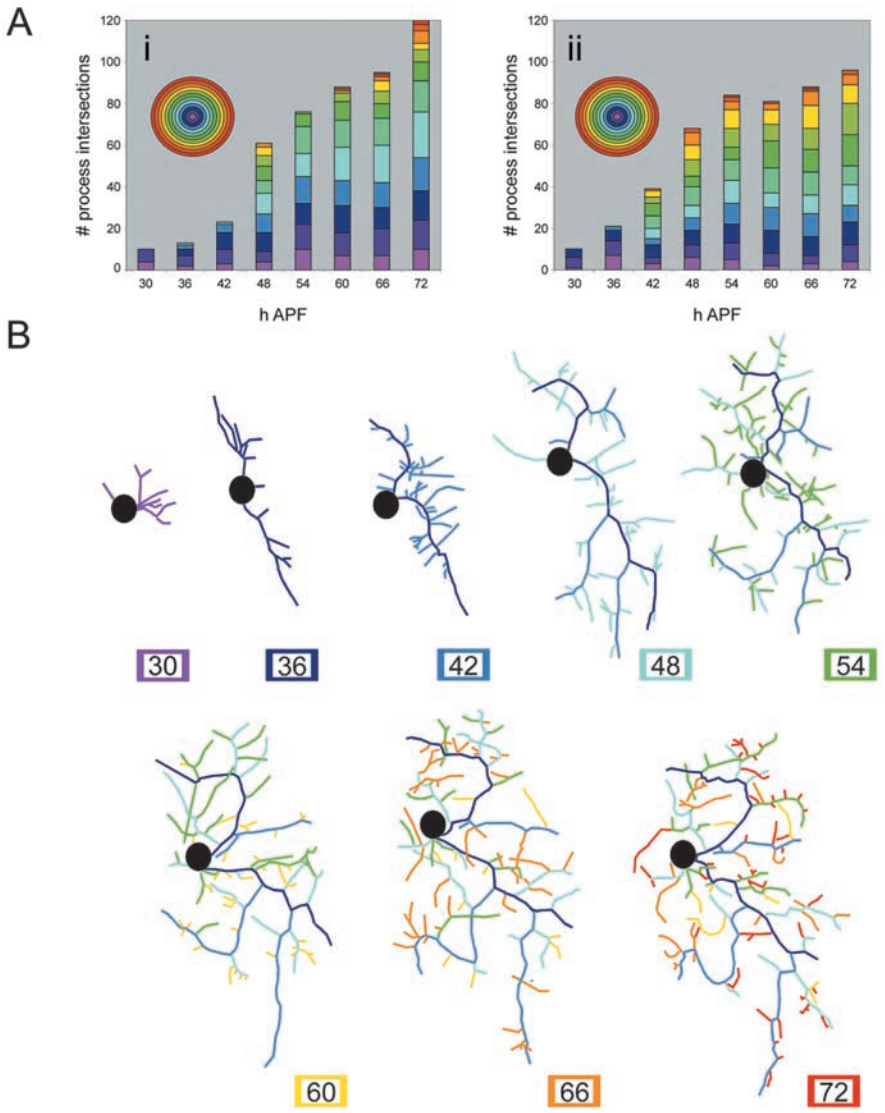

Figure 4. Quantification of outgrowth of adult dendritic arbor of ddaE. *A*, Sholl analysis of the dendritic arbor of two different ddaEs sampled every 6 hr between 30 and 72 hr APF. Acetone was applied at 24 hr APF. Individual time points are represented by columns. Each ring of the Sholl template is represented as a color of the spectrum on the histogram. *Aii*, Sholl data for the ddaE shown in *B*. Branch analysis of a single ddaE (data from multiphoton z-stacks are shown). Branches are assigned a color code when they are born and then retain it in all subsequent images.

Effects of a JH mimic on the metamorphosis of ddaE

Effects of time of JHm application

The developmental hormones 20E and JH are the two main developmental hormones that orchestrate molting and metamorphosis. The absence of JH during a molting peak of 20E results in a metamorphic molt. In *Drosophila*, as in other holometabolous insects, JH is not present during the pupal–adult transition (Riddiford, 1993). We applied JH mimic topically to prepupae and pupae at various times during metamorphosis and determined its effect on the formation of the dendritic arbor of ddaE, as assessed at 72 hr APF. Sholl analysis was performed on nine JHm-treated neurons and nine acetone-treated control neurons for each time point, and the data were averaged.

Figure 7*A* shows the appearance of ddaE at 72 hr APF after treatment with JHm at 0 hr APF. The hormone had a dramatic effect on the outgrowth of the adult arbor. Both the complexity and the size of the footprint covered by the arbor were severely reduced after the early JHm treatment. This can also be clearly seen in the Sholl analysis (Fig. 7*G,H*) for 0 hr APF treatment. JHm-treated neurons show a much lower number of process intersections, indicating lower complexity, and cross a reduced number of rings. When JHm treatment was delayed to 18 hr APF, ddaE also grew an arbor with reduced complexity, but it extended across the same size of the footprint covered by acetone control neurons (Fig. 7*B*). The Sholl data from these neurons show a reduced frequency of process intersections compared with the acetone control group, but the number of rings that are intersected is the same (Fig. 7*G,H*). The arbors therefore cover a similar area of the epidermis but do not "fill out" each Sholl ring with more branches. Similarly, JHm treatment at 24 hr APF (Fig. 7*C*) resulted in arbors that extended over the expected footprint but had approximately half the number of branch intersections as controls (Fig. 7*G,H*). By 30 hr APF, JHm treatments had no effect on the size or complexity of the arbor, as assessed at 72 hr APF (Fig. 7*D,G,H*). This is also seen for the last two treatments at 36 and 48 hr APF (Fig. 7*E–H*). No JHm treatments had any effect on the pruning of the larval arbors.

To ascertain whether the JHm treatments might be having a direct effect on the sensory neuron and/or its immediate environ-

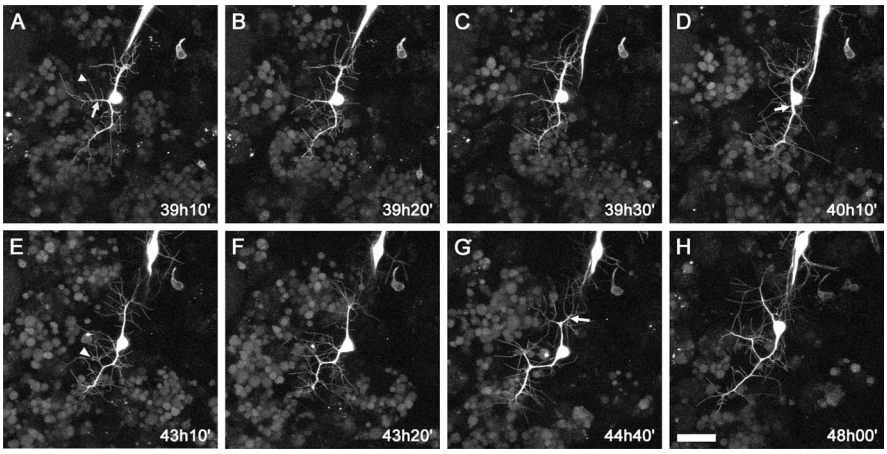

Figure 5. Dynamics of the early adult outgrowth of ddaE. Single frames from a multiphoton time-lapse movie of a neuron expressing the CD8::GFP reporter are shown. Acetone was applied at 24 hr APF. Samples were acquired every 10 min starting at 39 hr APF. The thin processes are filipodia and are distributed along the length of the primary dendrites. Branches are born at interstitial positions where filopodia have remained stable for a number of frames and generate growth cones. Between *E* and *F*, a thin process tipped with a growth cone becomes engorged with CD8::GFP (arrowhead). Substantial branches are labile at this early stage and may persist for ≥1 hr before they are removed. The left branch in *A* is lost within 1 hr (arrow). Similarly, the branch labeled in *G* (arrow) is lost ~3 hr later. Scale bar, 30 μm (also see movie 1, available at www.jneurosci.org).

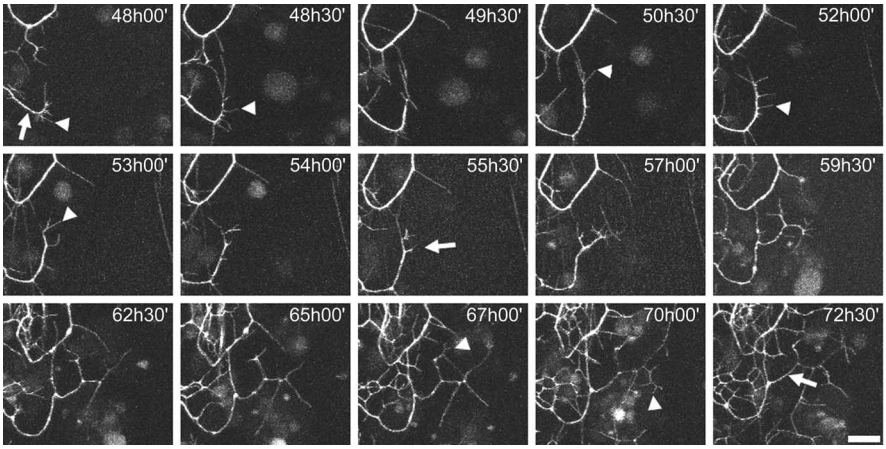

Figure 6. Dynamics of late adult outgrowth of ddaE. Single frames from a multiphoton time-lapse movie of a neuron expressing the CD8::GFP reporter are shown. Acetone was applied at 24 hr APF, and data points were collected every 30 min between 48 and 72.5 hr APF. Filopodia are evident in every frame of the movie (arrowheads denote examples). An arrow labels a branch in the first frame that remains stable until the end of the movie. A growth cone generates a new branch (55.5 hr APF) at a site where there has been filopodial activity. Once established, this new branch is stabilized, and higher-order branches are generated on it. No substantial branches are retracted through this period (also see movie 2, available at www.jneurosci.org). Scale bar, 15 μm.

ment versus a systemic effect, we applied JHm mixed in wax to the lateral region of the pupal cuticle overlying one-half of abdominal tergite 4. The wax was applied at 24 hr APF, and the arbor of ddaE was imaged at 72 hr APF on both the treated (Fig. 8*A*) and control (Fig. 8*B*) sides of the segment (Fig. 8). The cell on the control side (Fig. 8*B*) showed the normal extensive arbor of the adult form of ddaE, whereas the neuron on the JHm-treated side (Fig. 8*A*) was dramatically less complex. The same result was seen in two other animals that were so treated and indicates that the action of JHm on the dendrites of ddaE is local to the neuron and/or its immediate environment.

Effects of JH on outgrowth of ddaE

The JHm treatment at 0 hr APF resulted in adult neurons with severely stunted dendritic arbors. To establish how this early JHm treatment affected the growth of ddaE, we took time-lapse movies of the early growth of such cells (Fig. 9). Single frames from a movie taken between 39 and 45 hr APF show that the cell body of ddaE has migrated up the body wall and generated a growth cone covered with filopodia (Fig. 9, movie 3, available at www.jneurosci.org). The growth cone attempts to establish primary dendrites, but each nascent branch collapses. For the duration of the movie, no stable structures are generated. The final image in Figure 9 shows the same cell at 85 hr APF, by which time the cell had finally generated a few simple branches, representing <10% of the arbor generated by a normal cell.

The time-lapse data suggest that in the 0 hr-treated animals, ddaE is undergoing outgrowth, but strong retraction programs appear to coexist with the extension programs. To obtain greater resolution of the effects of JH on adult outgrowth, we examined animals treated with JHm at 24 hr APF. At this time, JHm treatment results in cells that have established an adult footprint but failed to fill it in with the normal density of branches. The progression of arbor formation of an individual ddaE in a JHm-treated individual is summarized in Figure 10. By 30 hr APF, the larval dendrites have been completely pruned, and the cell body of ddaE can be seen migrating dorsally along with the stretch receptor dbd. A number of filopodia can be seen extending from the soma (Fig. 10). At 36 hr APF, the cell body has nearly reached its final location on the body wall, and the growth cones are simple with numerous filopodia extending from short primary dendrites. Sholl analysis of the timeline data set from this neuron (Fig. 11*Ai*) and two others (Fig. 11*Aii,Aiii*) shows that at 30–36 hr APF, the neurons have the least number of processes and cover only a small area of the epidermis. The branch analysis (Fig. 11*B*) also demonstrates that most of the branches born between 30 and 36 hr APF are lost by the next time point.

Between 42 and 60 hr APF, the arbor undergoes a gradual increase in complexity and size (Figs. 10, 11*A*). The gradual increase in the number of rings crossed by the neuron in the Sholl analysis corresponds to the dendrites moving slowly over the footprint. Similarly, the gradual increase in the numbers of process intersections reflects a gradual increase in complexity.

The branch analysis shows that during this period, the majority of processes are unstable (i.e., not present in the final 72 hr APF image). This is striking in the 60 hr APF image (Fig. 11*B*), which shows the persistence of very few of the processes that were born at 48 and 54 hr APF.

At 66 and 72 hr APF (Figs. 10, 66–72 hr APF, 11*Ai,Aii*), the arbor reaches the edge of its normal footprint. The branch analysis shows that there are fewer branches from early developmental times, and that the majority of branches are born within 60–72 hr APF.

Dynamics of late growth in JHm-treated cells

The dynamics of the late growth of neurons treated with JHm at 24 hr APF were examined in greater detail with time-lapse microscopy starting at 48 hr APF. Figure 12 shows the details of such a movie. Filopodia are abundant and are present in every frame of this movie. Three branches emerge at 52 hr APF (branches A–C). By 58.5 hr APF, branch A has been lost. During the next few hours, a branch grows again at this site and is still present at 84 hr APF. Branch B is lost at 60.5 hr APF. Branch C grows to the edge of the target field until 64.5 hr APF and then collapses. By 72 hr APF, it was half of its maximum length, and by 84 hr APF, the branch was gone. These sequences are representative of events found in the two movies generated under these conditions. The dynamics of outgrowth seen in these later phases of metamorphosis of 24 hr APF JHm-treated pupae are characterized by high filipodial activity and the instability of both large and small branches (Fig. 12, movie 4, available at www.jneurosci.org).

Neurons from hormone-treated pupae also differ qualitatively from controls, in that during the latter half of metamorphosis filopodia are still found distributed along the entire length of lower-order branches (Fig. 13*D,F*). Over a period of 24 hr, 74 new filopodia were born along the length of the second-order branch shown in Figure 13*F*. In contrast, only one interstitial filopodium was seen in a control neuron during a comparable period.

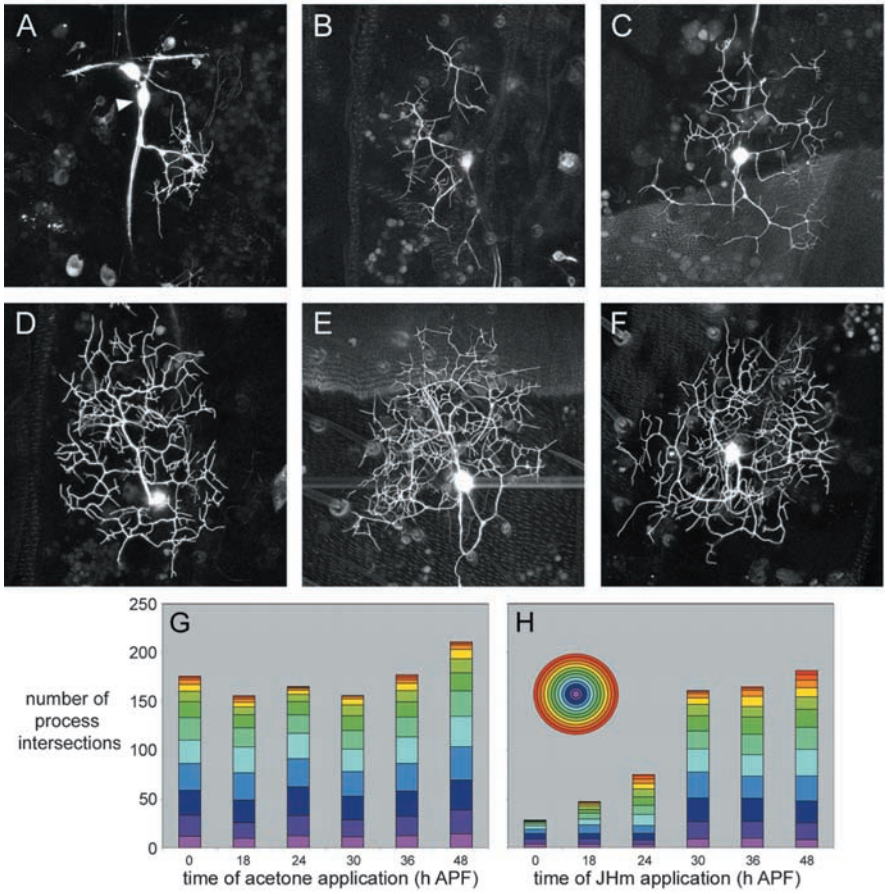

Figure 7. Effect of timing of juvenile hormone mimic application on ddaE arbor complexity. Projected confocal z-stacks of ddaE in 72 hr APF pupae expressing the CD8::GFP reporter are shown. The images of ddaE (*A–F*) are representative for the JHm treatment groups 0, 18, 24, 30, 36, and 48 hr APF, respectively. Scale bar, 45 μm. The arrowhead denotes ddaE. *G*, Sholl data for acetone control treatments. Each column represents the average Sholl data for nine neurons. *H*, Sholl data for JHm treatments. Each column represents the average Sholl data for nine neurons. Each ring of the Sholl template is represented as a color of the spectrum.

Discussion

Sensory neurons relocate by migrating on the body wall

The migration of neurons has been widely described in vertebrates (Hatten, 1999) but is less common in insects [e.g., migration of aCC and pCC in the grasshopper CNS (Bastiani et al., 1986) and of the enteric neurons (Horgan et al., 1994; Haase and Bicker, 2003)]. We report for the first time neuronal migration in the peripheral nervous system of *Drosophila*. After pruning back their dendrites, the persistent sensory neurons actively migrate to new positions on the body wall. (Figs. 2, 3).

The phases of adult dendritic outgrowth of ddaE

Shepherd and Laurent (1992) showed that local interneurons of *Shistocerca gregaria* generate their arbor in a stepwise manner, first with directed growth of the primary neurite across the midline followed by branching of the growth cone to generate a basic scaffold within the target field. This scaffold is then elaborated on with the expansive growth of higher-order branches. In the final step, outgrowth is curtailed and the arbor is refined, with discrete varicosities appearing at the site of predicted synapses.

The cell body of ddaE completes its migration between 36 and 42 hr APF and begins to establish the adult arbor with primary branches growing across the epidermis (Fig. 3). Sholl analysis shows that branches extend to the farthest extent of the sensory field between 42 and 48 hr APF. A number of the branches born during this period become stabilized as part of the adult form of the cell (Fig. 4*B*). After this extension phase, the number of intersections within individual Sholl rings increases, reflecting increased arbor complexity between 54 and 72 hr APF. Midline spiking interneurons undergo a similar increase in complexity late in embryonic development (Shepherd and Laurent, 1992).

The dynamics of the growth of ddaE showed at least two dis-

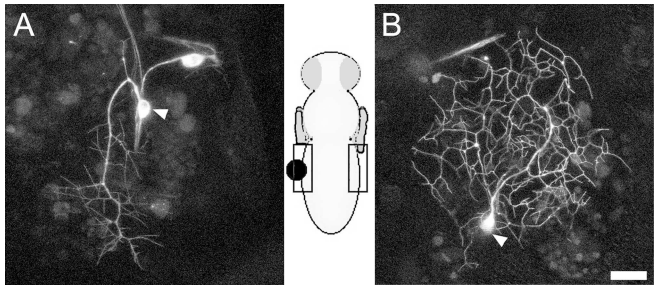

Figure 8. Local application of juvenile hormone mimic in wax. *A*, Projected confocal z-stack of ddaE expressing the CD8::GFP reporter imaged at 72 hr APF. Wax containing JHm was applied at 24 hr APF to the lateral region of the pupal cuticle overlying half of abdominal tergite 4 (see diagram). *B*, Projected confocal z-stack of ddaE from the opposite side of the pupa at 72 hr APF. Arrowheads denote ddaE. Scale bar, 45 μm.

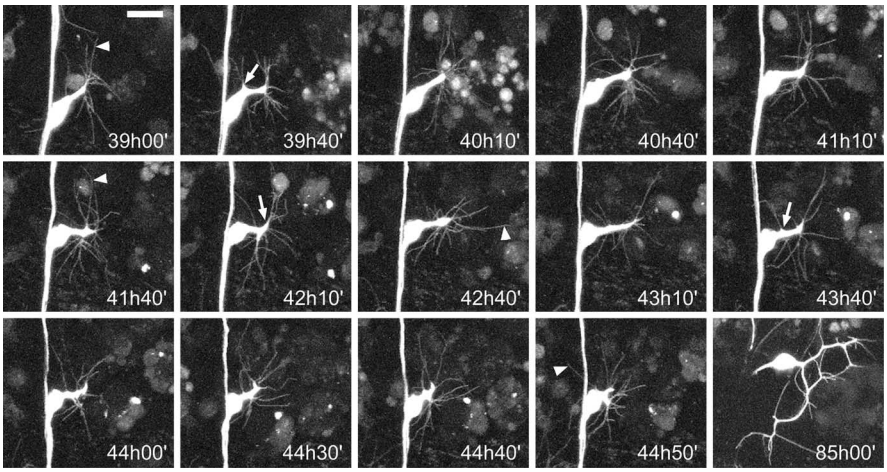

Figure 9. Dynamics of the early adult outgrowth of ddaE after JHm treatment at 0 hr APF. Single frames from a multiphoton time-lapse movie of ddaE expressing the CD8::GFP reporter are shown. JHm was applied at 0 hr APF. Samples were acquired every 10 min for 5 hr starting at 39 hr APF. The 85 hr APF image shows the simple arbor that is generated from such a treatment. The thin processes are filipodia (arrowheads). The protrusions on the growth cone (arrows) are attempts to generate branches, but all are retracted during the 5 hr movie (also see movie 3, available at www.jneurosci.org). Scale bar, 15 μm.

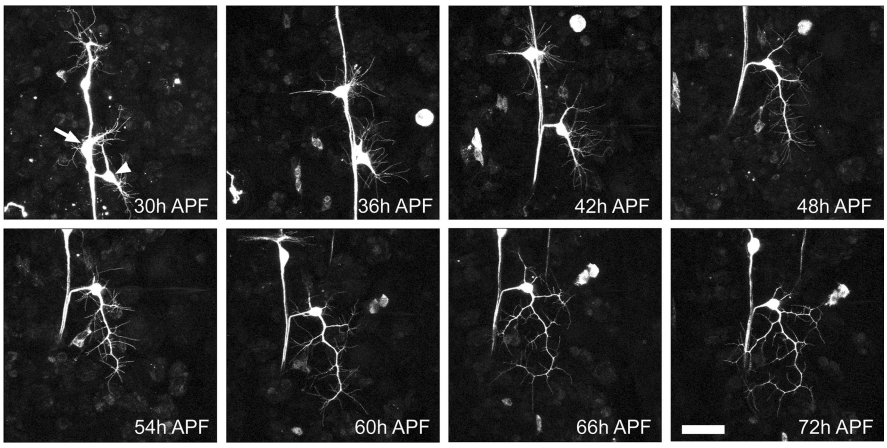

Figure 10. Effect of 24 hr APF juvenile hormone mimic application on adult outgrowth of ddaE. Projections of multiphoton z-stacks of ddaE expressing the CD8::GFP reporter are shown. JHm was applied at 24 hr APF, and ddaE was imaged at 6 hr intervals over the period from 30 to 72 hr APF. At 30 hr APF, the larval dendrites have been pruned, and the cell body of ddaE has migrated dorsally with the stretch receptor dbd. A number of filopodia can be seen extending from the cell body. At 36 hr APF, the cell body has numerous filopodia extending from short primary dendrites. Between 42 and 60 hr APF, the arbor undergoes a gradual increase in complexity and size. Between 66 and 72 hr APF, the arbor reaches the edge of its normal footprint. Arrow denotes dbd. Arrowhead denotes ddaE. Scale bar, 40 μm.

tinct phases of arbor construction. During the first phase (39–48 hr APF), growth is characterized by the presence of many protrusive filopodia and thin processes tipped with growth cones that extend and retract at a high frequency (Fig. 5). New branches are established at sites where filopodia have remained stable (Fig. 5*E–G*). Interestingly, when ddaE is in this scaffold-building stage, not only are thin processes retracted but more substantial primary branches are also labile. In the second phase of development, between 54 and 72 hr APF, filopodia and small growth cones are still labile, but larger branches are stable and never undergo retraction.

The growth dynamics of ddaE show many parallels with the growth of dendritic arbors of vertebrate neurons. The dendrites of rat pyramidal cells have filopodial extension and retraction cycles that take place on a minute time scale. Branches are initiated at sites where a filopodium forms a growth cone after being stable for a number of time-lapse frames (Dailey and Smith, 1996).

In vivo studies reveal that the dendritic growth of tectal projection neurons in *Xenopus laevis* can also be divided into distinct phases (Wu et al., 1999). In phase 1, neurons have differentiated and generated an axon but have a small dendritic arbor. During phase 2, the dendritic arbor of these projection neurons undergoes rapid outgrowth and major rearrangement, both adding and retracting branches. This mode of growth is very similar to that of ddaE between 39 and 54 hr APF as it generates its scaffold. During phase 3, the growth of the tectal projection neurons slows and the arbor becomes more stable, just as ddaE does in later development. In contrast to the dendrites described above, ddaE does not receive presynaptic input from other neurons. Studies on this neuron may therefore provide useful insights into intrinsic constraints on dendritic growth.

Application of juvenile hormone mimic during metamorphosis modifies dendritic growth

Although application of a JH mimic at metamorphosis is known to disrupt the gross anatomy of the nervous system in *Drosophila* (Restifo and Wilson, 1998), its effect on the growth of single identified neurons has not been reported previously. Knowing that JH is absent during the pupal–adult transition (Riddiford, 1993), we applied JHm to prepupae and pupae to explore how it would alter the growth of the arbor of ddaE.

As seen for other tissues in *Drosophila* (Zhou and Riddiford, 2002), JHm treatments did not suppress the larval–pupal transition, and ddaE shows a normal loss of its larval arbor despite treatment with JHm. However, early treatment with JHm does have dramatic effects on the size and shape of the final adult arbor (Figs. 7*A*, 9, 85 hr APF). Time-lapse data of the early outgrowth of ddaE in the 0 hr APF JHm treatment group showed that the cell is unable to establish branches, because nascent processes are retracted before they can be stabilized. The effect of the early JHm treatment on the growth of ddaE is complicated by the fact that the adult differentiation of the abdominal epidermis is also blocked (Zhou and Riddiford, 2002). Consequently, we turned to the effects of JH mimic applied at 18 and 24 hr APF, because these individuals make a normal adult cuticle.

In individuals treated with JHm at 18 and 24 hr APF, ddaE makes an adult-like arbor with markedly reduced complexity. In our analysis of the 24 hr APF JHm-treated ddaE, the arbor at 72 hr APF showed an under-representation of branches born between 48 and 54 hr APF compared with the acetone controls (Fig. 12*A–C*). Similar numbers of branches were born in both control and experimental groups at these times (data not shown), showing

that the under-representation is attributable to a reduced stability of branches in the JHm-treated neurons. (Figs. 4*B*, 11*B*). Time-lapse movies of neurons between 48 and 72 hr APF also show that the period of branch loss is prolonged in the treated group (Fig. 12, movie 4, available at www.jneurosci.org). A qualitative difference between the neurons of the two treatment groups also exists, with JHm individuals continuing to generate interstitial filopodia along the lengths of lower-order branches (Fig. 13*D–F*), suggesting a change in the stability of the cytoskeleton in these regions. Both the branch lability and the interstitial filopodia seen at late times in the treated neurons are features typical of the early, scaffold-building phase of arbor growth. Hence, it appears that neurons exposed to JHm fail to turn off some of the cellular processes that are features of their early phase of development.

A major developmental role of JH is to select the genes that will be expressed under ecdysteroid control (Zhou et al., 1998). The ability of early application of JH to suppress the adult differentiation of ddaE is not surprising and is consistent with similar JH treatments, causing the repetition of a pupal molt in tissues of many insects, including *Drosophila* (Zhou and Riddiford, 2002). The more intriguing results are seen with the later treatments (18–24 hr APF), in which the neuron establishes an adult-like arbor with reduced complexity. A similar quantitative effect of JH is also seen in remodeling motoneurons during early adult differentiation in *Manduca sexta* (Truman and Reiss, 1995). The latter motoneuron arbors showed reduced complexity but produced normal adult endplates, suggesting that these cells had undergone adult differentiation but with modified outgrowth. Because JH is normally not present during this period, its ability to exert a quantitative control over outgrowth may be a convenient endocrinological artifact. However, it is interesting that another group of neurons, the arrested adult-specific neurons, begin soma enlargement and adult outgrowth during the larval–pupal transition, a time when JH transiently reappears. Experimental manipulation of JH levels demonstrates that JH controls the amount of early growth shown by these cells in response to 20E (Booker and Truman, 1987). Consequently, the JH sensitivity shown by the adult-specific cells may also be shared by remodeling neurons during their outgrowth phase despite the fact that the latter neurons normally do not see JH at that time.

Our working model for how JH interacts with the developmental programs associated with remodeling emphasizes the maintenance of retraction processes during dendritic morphogenesis. The metamorphic transition begins with the removal of larval dendrites by pruning. For ddaE, as with mushroom body axons (Watts et al., 2003), dendrite removal occurs primarily by local degeneration, but retraction processes also appear to be involved in removing the proximal stumps (our unpublished observations). Branch loss by local degeneration is rarely seen in subsequent outgrowth, but branch retraction persists as a potent force. The changing emphasis on retraction versus extension programs may then allow the neuron to progress through the various stages of its outgrowth. Initially, the persistence of retraction programs after pruning would prevent the premature outgrowth of the cell during migration and allow the establishment of proper dendrite outgrowth sites. The reduction in the strength of retraction programs would permit outgrowth but provide the cellular machinery for establishing and refining the scaffold of the adult arbor. The final loss of the retraction programs then allows the filling out of the scaffold.

We suggest that JHm application maintains the retraction programs that are present at the time of application. We find that neurons blocked by 0 hr APF JHm application show intense filopodial activity, but retraction programs appear to dominate. This would reflect the retention of the retraction programs that were part of establishing the pupal form of the cell. For this early treatment, JH would be expected to have a "status quo" action

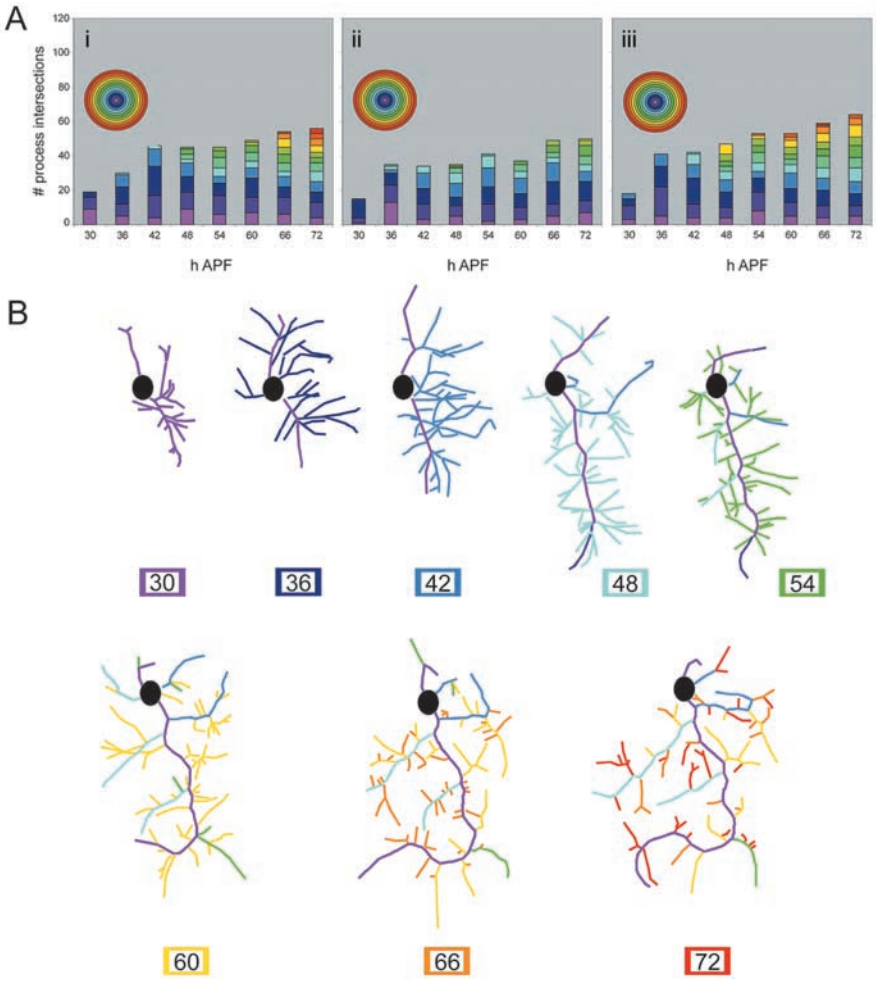

Figure 11. Quantification of the effect of 24 hr APF juvenile hormone mimic application on adult outgrowth of ddaE. *A*, Sholl analysis of the dendritic arbor of three different JHm-treated ddaEs sampled every 6 hr between 30 and 72 hr APF. JHm was applied at 24 hr APF, and ddaE was imaged at 6 hr intervals over the period from 30 to 72 hr APF. Individual time points are represented by columns. Each ring of the Sholl template is represented as a color of the spectrum on the histogram. Sholl data for *Ai* are from the neuron shown in Figure 10. *B*, Branch analysis of a single ddaE (data from multiphoton z-stacks shown in Figs. 10 and 11 *Ai*). Branches are assigned a color code when they are born and then retain that in all subsequent images.

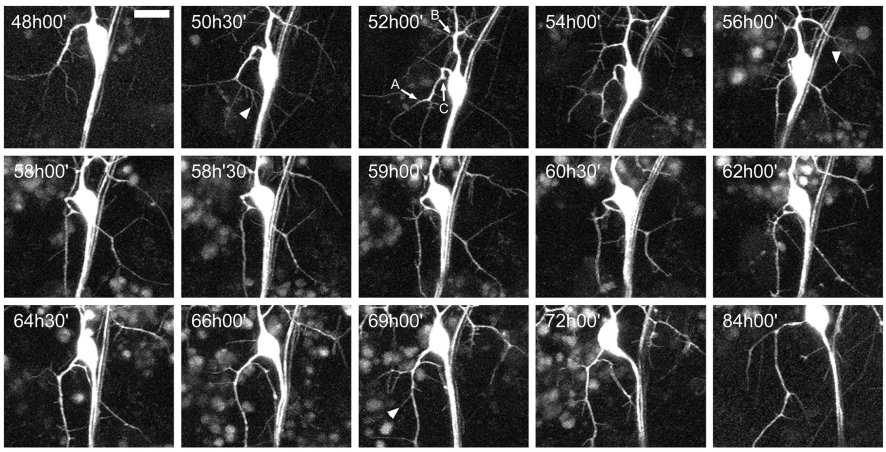

Figure 12. Dynamics of late growth in 24 hr APF JHm-treated cells. Single frames from a multiphoton time-lapse movie of ddaE expressing the CD8::GFP reporter are shown. JHm was applied at 24 hr APF, and ddaE was imaged every 30 min between 48 and 84 hr APF. Filopodia are evident in every frame of the movie (arrowheads denote examples). By 52 hr APF, three branches (A–C) were born (arrows). Branch A was lost by 58.5 hr APF. During the next few hours, a branch grew again at this position. By 69 hr APF, it became stable and was still present in the last frame of the movie. Branch B was lost at 60.5 hr APF and did not form again. Branch C continued to grow to the edge of the target field until 64.5 hr APF but collapsed. At 72 hr APF, it was half the length it was at 64.5 hr APF. Branch C was completely retracted by 84 hr APF (also see movie 4, available at www.jneurosci.org). Scale bar, 15 μm.

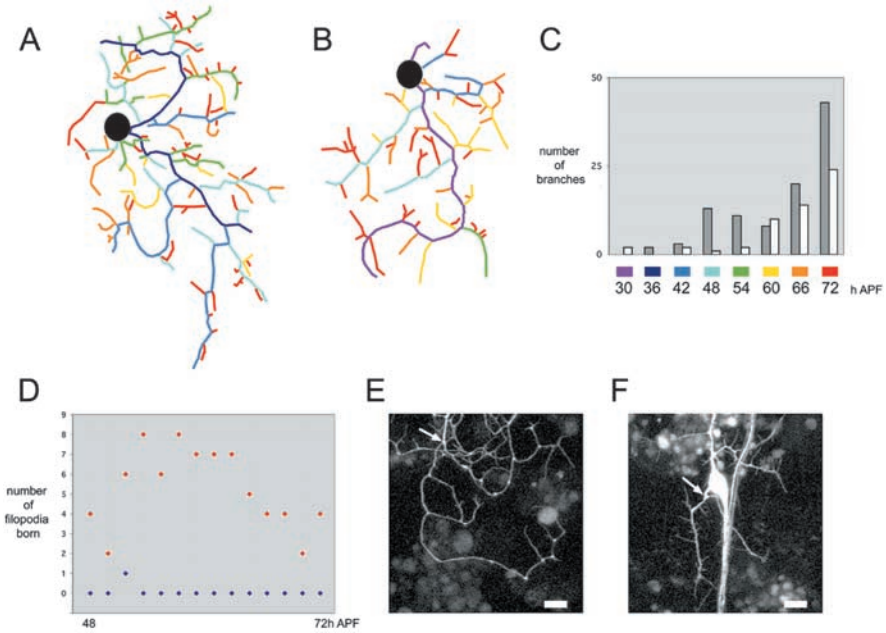

Figure 13. Comparison of quantitative and qualitative differences between JHm- and acetone-treated neurons. *A*, Final arbor of ddaE from branch analysis of the 24 hr APF acetone treatment group data set (Fig. 4*B*). *B*, Final tree of branch analysis of ddaE from the JHm 24 hr APF treatment group (Fig. 11*B*). *C*, Histogram summarizing the final trees of the branch analysis of 24 hr APF acetone control and 24 hr APF JHm treatment. The number of branches born at different time points are gray for acetone treatment (*A*) and white for JHm treatment (*B*). *D*, Summary of filopodia birth along a dendritic branch between 48 and 72 hr APF for individuals treated with acetone or JHm at 24 hr APF. Data were collected from multiphoton time-lapse movies of ddaEs expressing the CD8::GFP reporter. Blue diamonds indicate the number of filopodia born in an individual treated with acetone at 24 hr APF, and red diamonds indicate the number of filopodia born in an individual treated with JHm at 24 hr APF. *E*, Single frame at 63.5 hr APF of a multiphoton time-lapse movie of ddaE expressing the CD8::GFP reporter from an individual treated with acetone at 24 hr APF. Filopodia were counted along the length of the branch denoted with the arrow. Scale bar, 12 μm. *F*, Single frame at 63.5 hr APF from a multiphoton time-lapse movie of an individual treated with JHm at 24 hr APF. Filopodia were counted along the length of the branch denoted with the arrow. Scale bar, 12 μm.

(Riddiford, 1976; Levine et al., 1986; Weeks and Truman, 1986), suppressing to some extent adult extension programs, although this is difficult to assess considering the strength of the retraction present.

However, with later JH treatments, the extension program appears normal, at least when measured by the rate of birth of new dendritic branches, but retraction programs are maintained beyond their normal time. The morphology of neurons found after treatments at 18 and 24 hr APF suggests the incremental loss of retraction programs as development proceeds. Because there is a considerable precedent for JH affecting transcriptional programs (Riddiford, 1976; Zhou et al., 1998), we think it is likely that the treatment with JH may prolong the transcription of retraction-related genes. The closing of the window of JH sensitivity at ~30 hr APF might then indicate when these genes are normally shut off, but the persistence of their transcripts or proteins would then support retraction events that are evident until ~54 hr APF. The mechanism by which these retraction-related genes are normally shut off has not been determined, but it may be triggered extrinsically by the high titers of 20E that are experienced early in adult differentiation (before 36 hr APF). JH might prevent the high 20E titers from suppressing these genes in a manner similar to that proposed for the hormonal control of ventral diaphragm muscle development in *M. sexta* (Champlin et al., 1999). In the later case, low levels of 20E permit the proliferation of myoblasts, whereas high levels cause proliferative arrest and muscle differentiation. The presence of JHm allows 20E-dependent proliferation to be maintained even in the face of high 20E titers.

References

Bastiani MJ, du Lac S, Goodman CS (1986) Guidance of neuronal growth cones in the grasshopper embryo. I. Recognition of a specific axonal pathway by the pCC neuron. J Neurosci 6:3518–3531.

Booker R, Truman JW (1987) Postembryonic neurogenesis in the CNS of the tobacco hornworm, *Manduca sexta*. II. Hormonal control of imaginal nest cell degeneration and differentiation during metamorphosis. J Neurosci 7:4107–4114.

Champlin DT, Reiss SE, Truman JW (1999) Hormonal control of ventral diaphragm myogenesis during metamorphosis of the moth, *Manduca sexta*. Dev Genes Evol 209:265–274.

Dailey ME, Smith SJ (1996) The dynamics of dendritic structure in developing hippocampal slices. J Neurosci 16:2983–2994.

Gao FB, Brenman JE, Jan LY, Jan YN (1999) Genes regulating dendritic outgrowth, branching, and routing in *Drosophila*. Genes Dev 13:2549–2561.

Grueber WB, Jan LY, Jan YN (2002) Tiling of the *Drosophila* epidermis by multidendritic sensory neurons. Development 129:2867–2878.

Grueber WB, Jan LY, Jan YN (2003a) Different levels of the homeodomain

protein cut regulate distinct dendrite branching patterns of *Drosophila* multidendritic neurons. Cell 112:805–818.

Grueber WB, Ye B, Moore AW, Jan LY, Jan YN (2003b) Dendrites of distinct classes of *Drosophila* sensory neurons show different capacities for homotypic repulsion. Curr Biol 13:618–626.

Haase A, Bicker G (2003) Nitric oxide and cyclic nucleotides are regulators of neuronal migration in an insect embryo. Development 130:3977–3987.

Hatten ME (1999) Central nervous system neuronal migration. Annu Rev Neurosci 22:511–539.

Horgan AM, Lagrange MT, Copenhaver PF (1994) Developmental expression of G-proteins in a migratory population of embryonic neurons. Development 120:729–742.

Jan YN, Jan LY (2001) Dendrites. Genes Dev 15:2627–2641.

Kiehart DP, Montague RA, Rickoll WL, Foard D, Thomas GH (1994) High-resolution microscopic methods for the analysis of cellular movements in *Drosophila* embryos. Methods Cell Biol 44:507–532.

Komiyama T, Johnson WA, Luo L, Jefferis G (2003) From lineage to wiring specificity: POU domain transcription factors control precise connections of *Drosophila* olfactory projection neurons. Cell 112:157–167.

Lee T, Luo L (1999) Mosaic analysis with a repressible cell marker for studies of gene function in neuronal morphogenesis. Neuron 22:451–461.

Leuner B, Falduto J, Shors TJ (2003) Associative memory formation increases the observation of dendritic spines in the hippocampus. J Neurosci 23:659–665.

Levine RB, Truman JW, Linn D, Bate CM (1986) Endocrine regulation of the form and function of axonal arbors during insect metamorphosis. J Neurosci 6:293–299.

Miller FD, Kaplan DR (2003) Signaling mechanisms underlying dendrite formation. Curr Opin Neurobiol 13:391–398.

Rakic P, Sidman R (1973) Organization of cerebellar cortex secondary to deficit of granule cells in weaver mutant mice. J Comp Neurol 152:133–162.

Restifo LL, Wilson TG (1998) A juvenile hormone agonist reveals distinct developmental pathways mediated by ecdysone-inducible broad complex transcription factors. Dev Genet 22:141–159.

Riddiford LM (1976) Hormonal control of insect epidermal cell commitment *in vitro*. Nature 259:115–117.

Riddiford LM (1993) Hormones and *Drosophila* development. In: The development of *Drosophila melanogaster*, Vol II (Bate M, Martinez A, eds), pp 899–939. Cold Spring Harbor, NY: Cold Spring Harbor Laboratory.

Scott EK, Luo L (2001) How do dendrites take their shape? Nat Neurosci 4:359–365.

Shepherd D, Laurent G (1992) Embryonic development of a population of spiking local interneurons in the locust (*Schistocerca gregaria*). J Comp Neurol 319:438–453.

Shepherd D, Smith SA (1996) Central projections of persistent larval sensory neurons prefigure adult sensory pathways in the CNS of *Drosophila*. Development 122:2375–2384.

Sholl DA (1953) Dendritic organization in the neurons of the visual and motor cortices of the cat. J Anat 87:387–406.

Smith SA, Shepherd D (1996) Central afferent projections of proprioceptive sensory neurons in *Drosophila* revealed with the enhancer-trap technique. J Comp Neurol 364:311–323.

Trachtenberg JT, Chen BE, Knott GW, Feng GP, Sanes JR, Welker E, Svoboda K (2002) Long-term *in vivo* imaging of experience-dependent synaptic plasticity in adult cortex. Nature 420:788–794.

Truman JW, Reiss SE (1995) Neuromuscular metamorphosis in the moth *Manduca sexta*: hormonal regulation of synapse loss and remodeling. J Neurosci 15:4815–4826.

Usui-Ishihara A, Simpson P, Usui K (2000) Larval multidendrite neurons survive metamorphosis and participate in the formation of imaginal sensory axonal pathways in the notum of *Drosophila*. Dev Biol 225:357–369.

Watts RJ, Hoopfer ED, Luo L (2003) Axon pruning during *Drosophila* metamorphosis: evidence for local degeneration and requirement of the ubiquitin-proteasome system. Neuron 38:871–875.

Weeks JC, Truman JW (1986) Hormonally mediated reprogramming of muscles and motoneurons during the larval pupal transformation of the tobacco hornworm, *Manduca sexta*. J Exp Biol 125:1–13.

Williams DW, Shepherd D (1999) Persistent larval sensory neurons in adult *Drosophila melanogaster*. J Neurobiol 39:275–286.

Williams DW, Shepherd D (2002) Persistent larval sensory neurones are required for the normal development of the adult sensory afferent projections in *Drosophila*. Development 129:617–624.

Wu GY, Zou DJ, Rajan I, Cline H (1999) Dendritic dynamics *in vivo* change during neuronal maturation. J Neurosci 19:4472–4483.

Zhou B, Hiruma K, Shinoda T, Riddiford LM (1998) Juvenile hormone prevents ecdysteroid-induced expression of broad complex RNAs in the epidermis of the tobacco hornworm, *Manduca sexta*. Dev Biol 203:233–244.

Zhou XF, Riddiford LM (2002) Broad specifies pupal development and mediates the "status quo" action of juvenile hormone on the pupal-adult transformation in *Drosophila* and *Manduca*. Development 129:2259–2269.